Published in: J. Appl. Phys. **103** (2008) 034902

Ion-driven deuterium retention in tungsten

O.V. Ogorodnikova, J. Roth, M. Mayer[a)]

Max-Planck-Institut für Plasmaphysik, EURATOM-Association, Boltzmannstraße 2, D-85748 Garching, Germany

Abstract

The ion-driven retention of deuterium in polycrystalline tungsten (PCW) is studied experimentally and theoretically as a function of temperature, incident ion energy and ion fluence. Deuterium retention was investigated by thermodesorption spectroscopy and ion beam analysis. The peculiarities of deuterium behavior in PCW such as (i) ion-induced defect formation at low-energy implantation and (ii) higher D retention of low-energy ions (60 eV-200 eV) compared to high-energy ions (3 keV) at high fluences are considered. The effect of intrinsic defects (dislocations, vacancies, grain boundaries) and ion-induced defects (vacancies, dislocations, deuterium clusters) is discussed for polycrystalline tungsten.

[a)] Corresponding author

tel.: +49 89 3299 1639

e-mail: Matej.Mayer@ipp.mpg.de

1. INTRODUCTION

Tungsten, beryllium and carbon fiber composites are foreseen as plasma-facing materials for future fusion reactors. Although many studies concerning hydrogen retention and release in tungsten (W) have been performed [1-7], the behavior of implanted hydrogen isotopes in W is still not fully understood: The published data are often in disagreement and sometimes even contradictory. In the present paper, deuterium (D) retention in W is studied in a wide range of experimental conditions: various fluences, temperatures and energies. This allows a better understanding of the mechanism of hydrogen trapping and migration in tungsten.

By means of thermodesorption spectroscopy (TDS) after implantation combined with nuclear-reaction analysis, it is possible to measure both the total D inventory in a material and the D retention in the near-surface layer. This provides detailed information on the D migration and the types and distributions of defects responsible for trapping of deuterium. This paper will focus on the mechanism of deuterium diffusion and trapping during implantation of low- and high- energy deuterium ions in W.

2. EXPERIMENTAL

2.1. Specimen preparation

Two polycrystalline tungsten (PCW) materials of different purity (PLANSEE 99.96% and 99.99%), as proposed for ITER, were used. The dimensions of the samples were $12\times15\times0.5$ mm^3. The grain sizes were estimated from scanning electron microscopy (SEM) images to be in the range of 1-20 μm. All specimens were mechanically polished. Some of the specimens were electrochemically polished in 1 wt% NaOH aqueous solution (1wt% NaOH, 10V, Pt cathode, 2.5 minutes at room temperature). Before and after each electro-polishing step the samples were weighted on an analytical balance and the etching depth was estimated from the weight loss with an accuracy of about 40%. More than 0.5 μm of the surface layer was removed. The

uniformity of the electrochemical etching was controlled by SEM. Because each sample was used for several investigations, the previous implantation zone was removed with this polishing treatment. All samples were annealed at 1573 K for three hours in vacuum with a background pressure of 2×10^{-4} Pa before implantation. This temperature is high enough to remove any electro-polish residue from the surface, as well as some impurities, vacancies and dislocations in the near surface layer and to reduce the concentration of dislocations and grain boundaries in the bulk. This specimen preparation gives reproducible initial conditions before irradiation, and differences in the initial defect concentration from sample to sample are decreased with such high temperature pre-annealing. Prior to implantation the samples were outgased at 1273 K for 10 minutes in the implantation chamber with a background pressure of 10^{-6} Pa.

2.2. Deuterium implantation

Mass-analyzed deuterium implantations were performed in the Garching high current source using D_3^+ ions at normal incidence at a pressure of about 10^{-6} Pa. During implantation the pressure increases up to 10^{-5} Pa, mainly due to the partial pressure of the working gas. A liquid N_2 (LN_2) cold trap was installed in the target chamber to reduce the hydrocarbon and water partial pressures, thus minimizing the surface contamination during implantation. During the ion implantation the sample temperature was controlled by a pyrometer. The precision of the temperature measurement is about $\pm$ 50 K, mainly due to changes of the emissivity.

The tungsten samples were irradiated by D_3^+ with an energy of 600 eV, corresponding to 200 eV per deuteron and 6 keV D_2^+, corresponding to 3 keV per deuteron at normal incidence in the fluence range of $10^{21}\div5\times10^{24}$ D/m^2. The flux at the sample surface was about $2.5\div4\times10^{19}$ D/m^{2}s for low-energy implantation, increasing up to $8\div9\times10^{19}$ D/m^{2}s for high-energy implantation.

2.3. Thermal desorption spectroscopy (TDS)

The retention of implanted deuterium was investigated by TDS. The TDS experiments were performed in the same chamber as the implantations just five to ten minutes after the ion beam was switched off. Details can be found in [9, 10].

The samples were heated with a linear heating ramp at a rate of about 8 K/s using electron bombardment from the rear side. The maximum TDS temperature was 1373 K which was kept for 5-10 minutes at the end of the linear heating ramp. Deuterium desorption from the sample was detected with a calibrated Balzers 511 quadrupole mass spectrometer (QMS) at a base pressure of 10^{-7} Pa. To reduce the residual gas levels, especially of H_2O, the QMS is separately pumped and surrounded by a liquid nitrogen cooled copper shield.

The QMS signal was calibrated by implantation and subsequent thermal release of 3 keV D_3^+ in Ti at room temperature with a fluence of $F = 10^{22}$ D/m^2. Under these conditions, all non-reflected D is retained in Ti.

2.4. NRA measurements

Deuterium retention in the surface layer up to a depth of 800 nm was measured by the D(^{3}He,p)^{4}He nuclear reaction analysis (NRA) technique using ^{3}He ions with 1 MeV energy. The protons from the nuclear reaction were detected with a large angle counter. The NRA measurements were done 1-3 days and 2-6 months after deuterium implantation. The implanted samples were transported through air to the ion beam analysis chamber. To determine the D concentration at larger depths, an analyzing beam of ^{3}He ions with energies varied from 0.69 to 4 MeV was used.

3. RESULTS AND DISCUSSION

3.1. D^+ implantation into pure W

3.1.1. Influence of purity

To determine the influence of tungsten purity on deuterium retention, the implantation of 200 eV D^+ in two kinds of polycrystalline tungsten (*i*) pure W (99.96%) and (*ii*) extremely pure W (99.99%) was done. The results indicate that the small difference in purity of W does not influence the D inventory (Fig. 1). The same D retention was found for W (99.96%) and W (99.99%). The deuterium retention is about two times smaller compared to [9] due to the use of a more accurate calibration. Deuterium retention is observed to increase slightly faster than the square root of the incident fluence up to a fluence of $5x10^{24}$ D/m^2 for low-energy deuterium implantation in PCW at room temperature. The subsequent results presented in this paper were obtained with extremely pure tungsten W(99.99%)

3.1.2. Influence of implantation energy and fluence

In the fluence range of $10^{22} \div 5 \times 10^{24}$ D/m^2 no saturation of deuterium retention at 200 eV D^+ implantation was observed. Deuterium retention increases with incident ion fluence for low-energy deuterium implantation in PCW at room temperature (Fig. 2). In contrast, the retention of 3 keV deuterium increases slower and saturates at a fluence of 10^{24} D/m^2. In the present set up, the implantation of 3 keV D^+ in W is not possible at RT due to target heating by the incident ion beam. The temperature can rise up to 400 K depending on the ion beam density. The implantation of 200 eV D^+ at target temperatures between 380 and 470 K is also shown in Fig. 2 for comparison with the 3 keV deuterium implantation in the same temperature range. The deuterium inventory by 200 eV D^+ in the temperature range of 370-470 K increases much faster with ion fluence compared to 3 keV D^+ irradiation and does not saturate up to a fluence of 5×10^{24} D/m^2. The data scatter is partly due to uncontrolled sample heating by the incident beam during implantation and partly due to differences from specimen to specimen.

The retention of 3 keV D^+ is higher than the retention of 200 eV D^+ at low fluences up to 10^{23} D/m^2, because the 3 keV deuterium beam produces additional vacancies which can trap D and create

additional conditions for deuterium agglomeration in clusters. Therefore, most of the D is trapped near the implantation side. Moreover, 3 keV ions have a higher implantation range than 200 eV ions resulting in a higher D concentration in the implantation range because the diffusion path to the front side (from where the D is released) is longer for 3 keV. In addition, the reflection coefficient for 3 keV D^+ irradiation (r=0.417) is smaller than for 200 eV D^+ (r=0.56). The TDS spectra for a low implantation fluence of 10^{22} D/m^2 are shown in Fig. 3 for 200 eV and 3 keV deuterium implantations. Most of the low-energy deuterium implanted at room temperature is released from W at approximately 400 K, while the energetic deuterium implanted at 3 keV in W in the range of 380 K to 400 K has a release maximum at approximately 550 K. Deuterium is not retained in the traps with 400 K release temperature at 3 keV implantation due to the higher target temperature. A second release stage is observed at 550 K and 650 K for 200 eV and 3 keV, respectively.

The D inventory after implantation of 4 keV D^+ in PCW and 6 keV D^+ in single-crystalline tungsten (SCW) at low fluences was measured by Iwakiri et al. [11] and by Alimov et al. [4], respectively. These measurements also show a higher D retention with increasing ion energy, in agreement with our measurements.

Fig. 4 shows thermodesorption spectra after implantation of low- and high- energy D ions at high fluences, $F \geq 10^{24}$ D/m^2. The amount of D released in both TDS peaks is still increasing with fluence during 200 eV implantation. For 3 keV implantation the amount of D released in the two peaks is not further increased. The retention of 200 eV deuterium at RT is higher than for 3 keV at T~400 K.

Deuterium retention by irradiation with 3 keV D^+ at moderate tungsten temperatures of 440-480 K is smaller compared to T~400 K, but the deuterium inventory increases faster with ion fluence and does not show saturation in the investigated range of fluences (Fig. 5). The same temperature effect has been demonstrated above (Fig. 2) for 200 eV D^+ irradiation. Several key observations can be made from the TDS experiments:

- Higher D retention for 3 keV D^+ implantation than for 200 eV at low fluences.
- Lower D retention for 3 keV D^+ irradiation than for 200 eV at high fluences.
- The D retention increases with ion fluence for 200 eV D^+ at room temperature as $\sim F^{0.7}$ and does not saturate up to a fluence of $F > 5 \times 10^{24}$ D/m^2.
- The D retention saturates with fluence at a fluence of $F = 10^{24}$ D/m^2 for 3 keV D^+ at ~400 K. If at all, then the D retention saturates only at a much higher fluence of $F \geq 10^{25}$ D/m^2 for 200 eV D^+.
- The D retention decreases with increasing temperature at low fluences. For the highest fluences the difference in the retention by increasing the temperature from 300 K to 400 K decreases.
- The D retention increases faster with ion fluence at elevated irradiation temperatures (~400 K for 200 eV D^+ and ~450 K for 3 keV D^+) compared to near-room temperatures.

As was shown by nuclear reaction analysis (NRA) within a probed depth of about 800 nm, most of the deuterium is trapped in the bulk of the W at high fluences (see Fig. 1). The deuterium content decreased by 15% after 720 hours (1 month) exposure of W to air after implantation. The samples were stored at room temperature. This indicates that most of the deuterium is trapped with a trap energy which is high enough to prevent deuterium release at room temperature.

3.1.3. Modeling

The retention of D ions in metals is characterized by the speed of implantation (i.e. the implanted flux density) and the speed of diffusion (i.e. the diffusivity). Moreover, implanted ions create radiation defects such as Frenkel pairs, clusters of defects and dislocations. The behavior of implanted D strongly depends on the rate of displacement radiation damage during the implantation [12]. These processes strongly influence the binding energy and the diffusion of D in the lattice. The other factor influencing the D migration is the implantation energy. The deeper D

penetrates into a solid, the deeper surface modifications take place. Moreover, a stress field created by the irradiation can influence the deuterium diffusion and defect development.

Deuterium migration in metals is described by a diffusion equation with an ion source term and trapping in various defects [9]. In the case of low-energy implantation two kinds of traps were found for low irradiation temperatures [9]: (i) low-energy traps with a trapping energy of 0.85 eV, and (ii) high-energy traps with a trapping energy of 1.45 eV. The low-energy traps were identified as dislocation sites and grain boundaries. The high-energy traps were found to be D agglomeration in clusters in the form of D_2 molecules and D trapping in vacancies [4, 9]. The different energies of deuterium to be released from W are summarised in Table 1. Due to the small difference in the trapping energy of a deuterium atom trapped in a vacancy and the trapping energy of deuterium molecules in microvoids or microcavities [13-16], it may be difficult to resolve these two trap sites experimentally. On the other hand, TDS measurements influence the initial D distribution by annealing. According to [17], already at approximately 600 K the vacancies become mobile and can form vacancy clusters. D can be released and re-trapped by a different trap site than it was initially trapped. Atomic D can also agglomerate in clusters by diffusion through interstitials during annealing. These processes concur with D dissociation from clusters. Therefore, because D can be released at similar temperature from bubbles created during implantation, from bubbles created during TDS annealing and from vacancies, TDS measurements alone cannot give a definitive conclusion about the nature of the traps and the initial deuterium distribution in the traps. Only the trap energies and defect distributions can be accurately determined by TDS. Additional depth profile measurements are helpful but not always conclusive on the nature of deuterium low-temperature and high-temperature trap sites due to the complication of D release from vacancies and voids at the same temperature.

Calculations using a diffusion model with low-energy 'natural' defects distributed over the whole thickness of the sample, and high-energy 'ion-induced' defects distributed near the implantation surface and growing during the implantation, describe well the experimental data for 200 eV D^+ [9]. The increase of the trap density, *W*, with fluence can be written in analogy to spontaneous recombination of defects in metals [18]:

$$dW/dt = (1-r) I_0 \psi(x)(1-\eta W/W_m) \ , \qquad (1)$$

where I_0 is the incident flux, r is the reflection coefficient, ψ is the depth distribution of ion-induced defects, η is the rate of the defect creation and W_m is the maximal defect concentration. From Eq. (1) the trap density increases with time, *t*, as follows

$$W(x,t)=W_m(1 - \exp(-(1-r)I_0 \psi(x) \eta \, t/W_m)). \qquad (2)$$

A more detailed modelling for both TDS and depth profile experiments shows that not only the amount of high-energy traps increases with fluence, but also the concentration of low-energy traps can rise near the implantation range during irradiation. However, the concentration of ion-produced high-energy traps is higher than the concentration of ion-induced dislocations in the near surface layer (Table 2), especially for 200 eV D^+ implantation. Calculations using the model [9] and Eq. (2) show that the high-energy traps are distributed in a thin surface layer which is about 50-100 nm thick, while low-energy ion-induced traps can be distributed up to several thousands nm (Fig. 6). Similar depth profiles were found experimentally by Alimov at al. [19] (Fig. 7). Calculations using the parameters presented in Table 2 describe very well the TDS experiments (see Figs. 3 and 4).

As already described, the trap concentration grows with fluence. But also the ion-induced defect distribution propagates into the bulk of the target. According to van Veen [15] and Nagata [20], the ion-induced damage can extend many times deeper than the implantation depth. The diffusion in the damage zone can differ considerably from the bulk diffusion.

As calculations show (see Table 2 and Figs. 2-4), the range of the defect profile is five times larger than the implantation profile for low fluences (such as $F=10^{22}$ D/m^2), while it is hundred times

larger for high fluences (such as $F=10^{25}$ D/m^2). This is because of the expansion of the stress field during the exposure time. Although there has been no general theoretical or experimental study of the effect of stress on defect dynamics, we can conclude that the tensile field provokes the production of extended defects such as dislocation loops.

3.1.3.1. Peculiarity at low-energy implantation: nature of low-energy ion-induced defects

The calculated fluence dependence of D retention, using a diffusion model with intrinsic and ion-induced trap parameters presented in Table 2 for non-activated desorption, is shown in Fig. 2 for 200 eV D^+. The calculations describe the experimental data for low-energy implantation well (see also Figs. 3 and 4). The amount of deuterium in pre-annealed polycrystalline W decreases with temperature in agreement with the experiments, as shown in Fig. 8. The experimental data of deuterium in W measured at various irradiation temperatures by the NRA method up to 6 μm in poly-crystalline W (PCW) [19] and by the TDS method in single crystalline W (SCW) [21] are also shown for comparison. All data show the same tendency: a reduction of the deuterium concentration in W with temperature up to a fluence of $F=10^{24}$ D/m^2. Since NRA allows measuring only the deuterium near the implantation side up to a limited depth, the total amount of D is significantly underestimated compared to TDS, especially at elevated temperatures and long-time implantation when more D diffuses into the bulk of the sample.

According to TRIM calculations [22], 200 eV D^+ cannot produce vacancies in W due to the small energy transfer. However, to describe the TDS spectra, it is necessary to assume some ion-induced defects near the surface. To describe the experimental data of low-energy implantation at room temperature by the modeling of just natural defects, two types of traps with trapping energies of 0.9 eV and 1.2 eV and trapping densities of $W=10^{-3}$ at.fr. and $W=6\times10^{-4}$ at.fr., respectively, have been used. However, the calculations using only ‘natural’ traps of 0.9 eV and 1.2 eV distributed uniformly over the W thickness are in disagreement with

experiments: the model with only ‘natural’ traps results in an increase of the deuterium content in W with temperature, while in the experiments the deuterium inventory in pre-annealed W decreases with irradiation temperature (Fig. 9). Additional arguments for the presence of ion-induced defects are that the calculated TDS spectra using only ‘natural traps are broader than in experiments and calculated TDS peaks show a more pronounced shift to high temperatures with fluence compared to the experiment. Moreover, calculations with only intrinsic defects do not describe the experimental depth profiles at all as one can see from Fig. 10: the calculated profile is flat and does not strongly decrease with temperature. Concerning to the calculated parameters without an assumption of ion-induced defects, the concentration of intrinsic traps should be 10^{-3} at.fr. in order to have an agreement with experimental data which is quite high for tungsten.

These assumptions leave open questions: What is the nature of these ion-induced defects? What is the nature of the modified near-surface region? And why does the surface layer differ from the bulk? Possible explanations can be the following:

1) In [23], it was found that D^+ irradiation of single crystalline tungsten (SCW) at the Toronto ion beam facility creates near surface peaks in the C and O depth distributions. It was proposed that impurities from the residual gas are implanted into W by recoil collisions with the incident D^+ ions and can create vacancies in W in the near-surface region. Such vacancies can be centres of deuterium inventory and, consequently, for D agglomeration in clusters.

2) We propose another mechanism of ion-induced defects production: The high D inventory near the surface arises from deuterium agglomeration in clusters due to a stress field induced by the incident ion flux. Such clusters can contain deuterium molecules. One possible mechanism can be the following: D can be trapped in lattice defects such as dislocations, vacancies, grain boundaries or other crystal defects within the implantation zone. Let the D be trapped by a vacancy. If the incident flux is higher than the rate of D diffusion out of the implantation range, all traps will be filled with D. Due to the low solubility of D in W, a local super-saturation of D

is reached. Then, the next D atoms can also be retained in this already occupied vacancy. High D concentration near a surface results in tensions and stresses. Several D atoms in a single vacancy can cause the displacement of neighbouring lattice atoms, creating a di-vacancy and thus initiate bubble growth. Fig. 11 illustrates the mechanism of D cluster growth due to stress-induced atomic diffusion. The stress field around an interstitial atom in a solution can be so strong that the atom can be attracted to a dislocation. Moreover, dislocations can be also produced by the stress field created by implanted deuterium. Consequently, with increasing D concentration lattice atoms near D clusters re-construct in such a way that free traps for D atoms are created in order to reduce the mechanical tension. On the other hand, tensions arising near the surface delay the movement of dislocations to the surface in the case of PCW for unmovable grains and, consequently, result in an inventory of dislocations near the surface. These dislocations can trap D and retard D migration, and can result in additional D agglomeration in molecules and bubbles. The tension field can even prevent migration of D into the tungsten bulk. But at high concentration of dislocations (for example, for 3 keV irradiation), they can enter on the surface and increase the D desorption by increasing the diffusion coefficient.

Consequently, ion-induced defects are produced by the tension field in the case of low energy bombardment. Self-aggregation due to the stress field induced by the incident ion flux results in bubble formation without pre-existence of radiation-induced vacancies. Tension and stresses result in the creation of deuterium clusters in a surface layer many times deeper than the implantation range. The stress field increases with increasing ion flux or fluence.

3.1.3.2. Peculiarity at high-energy implantation: a change of the diffusion mechanism in the near the implantation side

In addition to the previously described mechanism, D is trapped in ion-induced vacancies generated within the implantation range by sufficiently energetic ions. Thus, the D retention is

higher for 3 keV than for 200 eV at low fluences. However, with increasing fluence the D retention reaches saturation faster than at 200 eV D^+ implantation.

The difference between 3 keV deuterium implantation and 200 eV D^+ is that energetic ions (i) penetrate deeper into material and (ii) create defects such as vacancies near the implantation side.

The deeper penetration of 3 keV deuterium ions results in a higher D concentration in the implantation range. High-energy ions create vacancies. The threshold energy for vacancy formation by deuterium implantation is 1030 eV. The generation of vacancy type defects likely creates dislocation loops, as observed by Sakamoto et. al. [24]. The stress field causes the lattice distortions which are extended to a larger depth compared to the defect distribution calculated by the TRIM-code. The defects generated by 3 keV deuterium ions are additional centers for deuterium trapping. Consequently, deuterium retention for 3 keV ions is higher than for 200 eV at low fluences. The model taking into account the higher rate of defect production for 3 keV ion irradiation describes well the low fluence deuterium retention in PCW for 3 keV D^+. The reduction of the saturated concentration of high-temperature traps is explained by the agglomeration of vacancies in voids. Thus, the density of voids is less than vacancies. Since, at such a low temperature as 400 K the vacancies in W are still immobile [13], the formation of voids at 400 K is due to the stress field induced by energetic ions. This means that the stress-induced field results in an agglomeration of vacancies in voids and a production of dislocations during implantation even at such a low temperature as 400 K. The reduction of the bubble density with increasing ion energy was also observed by Sakamoto et al. [24]. Even as a void has a bigger size than a vacancy, the D concentration seems not to increase significantly with increasing bubble size. As a result, the maximum density of high-temperature defects for 3 keV D^+ is smaller than the density of high-temperature defects for 200 eV D^+.

Although the model presented in Table 2 describes well the low fluence deuterium retention in W irradiated by energetic ions, the model overestimates the D retention at high fluences (solid stars in

Fig. 5). Also, the model does not describe the saturation behavior for 3 keV D^+ irradiation at fluences above 10^{23} D/m^2. This can be due to several reasons:

1. The permeation of D through the sample can decrease the D content in W.

2. D can be trapped with high binding energy, requiring release temperatures above the maximum of the TDS temperature of 1373 K.

3. An increase of the near-surface diffusion coefficient within the implantation range with fluence due to the creation of open porosity and a dislocation network which helps D to be easily released from the material.

4. An increase of the diffusion coefficient near the surface or a reduction of the diffusion coefficient inside the W bulk due to a tension field which prevents deuterium to move into the bulk.

Permeation through the sample or D trapping with extremely high trap energy (T>1373 K) are not responsible for the disagreement of experiments and calculations. NRA shows a negligible D concentration on the outlet side compared to the inlet side. That indicates that the loss of deuterium due to permeation through a 0.5 mm thick W is small. The D release from traps with T>1373 K was not observed using higher temperatures of TDS.

To check if an increase of the diffusion coefficient in the implantation range is the reason for the lower D retention in PCW for 3 keV D^+ irradiation compared to 200 eV D^+ irradiation at high fluences, calculations have been performed. Fig. 12 shows the assumed increase of the diffusion coefficient near the implantation side. It varies with fluence according to the equation:

$$D(x,t) = D_m(1-(1-D/D_m)\exp(-(1-r)I_0\psi(x)\eta t/u_m) \ , \qquad (3)$$

where D_m is the maximum diffusion coefficient in the implantation range. This equation for ion-induced diffusion is written in analogy to the increase of trapping sites in the implantation range during the implantation (see eq. (2)). To describe the deuterium behaviour in W under energetic ion irradiation, both an increase of the diffusion coefficient in the implantation range with

fluence, and an increase of the rate of the defect production, η, are suggested. The calculations results in saturation behaviour of 3 keV D^+ implantation at fluences of 10^{24} D/m^2 as observed in the experiment (solid squares in Fig. 5).

A surface modification by 3 keV D^+ irradiations has been observed by SEM (Fig. 13). Indeed, 3 keV D^+ irradiation changes the surface morphology by creating bubbles inside the grains which are visible by SEM. Some traces of the plastic deformation have been observed as etching pits with a size of ~0.1-0.3 μm inside the grains. The etching pits can be a result of preferential sputtering of W atoms near vacancies clusters or dislocation loops entering on the surface from the bulk. No significant microstructural changes were observed by irradiation with D^+ ions of 200 eV up to a fluence of 10^{24} D/m^2.

The last question which should be clarified is: if an increase of the diffusion coefficient in the sub-surface layer during high-energy ion implantation is connected with (i) *the damage process*, namely porosity and a dislocation network development which helps D to be easily released from the material or (ii) *due to ion-induced stress field* created by D ion irradiation.

To answer this question, a pre-implantation with 3 keV D^+, following by deuterium release by TDS and subsequent implantation of 200 eV has been done. If the increase of the diffusion coefficient near the surface is connected with *the damage process* (porosity development, etc.) then the subsequent implantation of 200 eV ions after the damaging process should also result in a saturation of the retention at relatively low incident fluences of 10^{24} D/m^2. However, the surface modifications by 3 keV deuterium irradiation do not essentially influence the 200 eV retention at high fluences: no saturation is observed in the investigated range of fluences (Fig. 14). This means that the damages in the near of the implantation depth produced by high energy ion pre-implantation do not influence the diffusion coefficient. Moreover, the amount of D retained in the sample after 3 keV D^+ pre-implantation is higher compared to the case without pre-implantation at low fluences (10^{22} D/m^2). This can be explained by taking into account that

ion-induced defects created during the pre-implantation are not annealed by TDS up to 1373 K [13]. Consequently, the increase of the diffusion coefficient near the implantation side *by the damage process* is not the reason for the saturation behaviour of the 3 keV deuterium ions irradiation. On the basis of this study, one can conclude that neither open porosity nor formation of a dislocation network influence the diffusion coefficient near the implantation side. The diffusion coefficient can be changed near the surface *due to a stress field* induced by the incident ion flux. Thus, the high concentration of D itself in W can cause the change of the diffusion coefficient, but not internal porosity as usually postulated. Under the implantation of 200 eV D^+, deuterium diffuses far beyond the implantation range in PCW. Under the implantation of 3 keV D^+, most of the D is accumulated in the surface layer of 10 μm as our calculations show (Fig. 15). For 200 eV D^+ the stress field is not as strong as for 3 keV D^+, and does not influence the diffusion coefficient.

3.1.3.3. High-temperature implantation: application to ITER

Concerning to deuterium retention in fusion reactors, tungsten is foreseen to be used at temperatures above 600 K. At irradiation temperatures of 673-873 K, vacancies became mobile. They diffuse, some of them annihilate with interstitials, some disappear on the grain boundaries and on the surface and some agglomerate to form vacancy clusters with up to 60 vacancies [13]. In the case of high-temperature irradiation, D can be retained in W only by chemisorptions on the internal walls of such voids due to the high binding energy of deuterium atoms with micro-voids (see Table 1). Indeed, a high-temperature peak at temperatures between 800 and 1200 K is observed in the TDS curves (Fig. 16). As our calculations show, the essential amount of deuterium will be retained in traps with energy of 2.1 eV at high irradiation temperatures. This kind of traps corresponds to D chemisorptions inside the ion-induced micro-voids, namely chemisorptions on the bubble wall [15]. For the investigated irradiation temperature range of

300-500 K in the present paper, the amount of deuterium in the peak of 1000 K (2.1 eV) is negligible compared to the retained D in the two other peaks. The influence of this third peak on the D inventory in PCW becomes only important at elevated irradiation temperatures above about 600 K.

4. CONCLUSIONS

Ion-driven retention of deuterium in tungsten has been studied by means of thermal desorption spectroscopy (TDS) combined with nuclear-reaction analysis. Experiments made at the Garching ion source facility showed several features of deuterium interaction with tungsten:

1) The retention of low-energy deuterium in polycrystalline W is higher than the retention of energetic deuterium at high fluences $>10^{24}$ D/m^2.

2) Faster increase of D retention with fluence for high temperature irradiation compared to room temperature implantation.

3) Pre-implantation followed by thermal D release and subsequent low energy implantation results in higher D retention in W.

Modeling shows the presence of ion-induced and natural defects in polycrystalline W which act as trap sites for deuterium. Ion-induced defects are produced during implantation by deuterium self-aggregation due to the stress field induced by the incident ion flux. The rate of ion-induced defect production depends on the energy of the incident ions, ion flux, target temperature and exposure time. The defects production rate increases with the energy (and/or ion flux) and temperature.

A reduction of the saturated density of ion-induced traps was found for 3 keV D^+ compared to 200 eV D^+. One reason may be the agglomeration of vacancies and bubbles in voids. Since the trap energies of D_2 in voids, deuterium in clusters, and atomic deuterium with vacancies are almost identical around ~1.4 eV, the agglomeration of vacancies in voids could decrease the maximum high-temperature trap concentration with ion energy. Although the vacancies are immobile at implantation temperatures of 400-500 K, the stress-induced field can initiate growth of voids. However, only the reduction of the maximum defect density does not describe well the lower value of retained deuterium for 3 keV D^+ compared to 200 eV D^+ irradiation *at high fluences*.

To explain the lower D inventory in W by energetic ions implantation compared to low energy deuterium ions, a stress-induced change of the diffusion coefficient is suggested. This model yields

a good agreement with experimental data and it can describe simultaneously TDS spectra, the energy, fluence and temperature dependences of the retained D amount, and the deuterium depth profiles with the same set of parameters. Further experimental investigations are needed to fully understand the influence of the stress field on the diffusion mechanism of deuterium and agglomeration in clusters in various tungsten materials for different incident ion energies and irradiation temperatures.

Acknowledgement

We would like to thank A. Weghorn for the technical assistance and S. Lindig for the SEM investigations.

References

[1] M. Poon, A.A. Haasz, J.W. Davis, R.G. Macaulay-Newcombe, J. Nucl. Mater. 313-316 (2003) 199.

[2] R. Causey, J. Nucl. Mater. 300 (2002) 91.

[3] R. Causey, K. Wilson, T. Venhaus, W.R. Wampler, J. Nucl. Mater. 266-269 (1999) 467.

[4] V. Kh. Alimov, A.P. Zakharov, R. Kh. Zalavutdinov, 'Hydrogen and Helium Recycling at Plasma Facing Materials'. Ed. A. Hassanein, NATO Science Series II, Kluwer Academic, 2001, v. 54, p. 131.

[5] P. Franzen, C. Garcia-Rosales, H. Plank, J. Roth, V. Kh. Alimov, J. Nucl. Mater. 241-243 (1997) 1082.

[6] R.A. Anderl, R.J. Pawelko, S.T. Schuetz, J. Nucl. Mater. 290-293 (2001) 38.

[7] R.A. Anderl, D.F. Holland, G.R. Longhurst, R.J. Pawelko, C.L. Trybus and C.H. Sellers, Fusion Technology 21 (1992) 745.

[8] M. Balden, E. Oyarzabal, E. De Juan Pardo, K. Durocher, J. Roth and C. Garcia-Rosales, Physica Scripta, v. T103 (2003) 38.

[9] O.V. Ogorodnikova, J. Roth, M. Mayer, J. Nucl. Mater. 313 (2003) 469.

[10] W. Eckstein, C. Garcia-Rosales, J. Roth and W. Ottenberger, Sputtering data, Tech. Rep. IPP 9/82, Max-Planck-Institut fuer Plasmaphysik, 1993.

[11] H. Iwakiri, K. Morishita, and N. Yoshida, J. Nucl. Mater., 135-138 (2002) 307.

[12] R. Sakamoto, T. Muroga, N. Yoshida, J. Nucl. Mater. 220-222 (1995) 819.

[13] H. Eleveld and A. van Veen, J. Nucl. Mater. 212-215 (1994) 1421.

[14] H. Eleveld and A. van Veen, J. Nucl. Mater. 191 (1992) 433.

[15] A. van Veen, H.A. Filius, J. de Vries, K.R. Bijkerk, G. J. Rozing, D. Segers, J. Nucl. Mater. 155-157 (1988) 1113.

[16] J. B. Condon and T Schober, J.Nucl.Mater., 207 (1993) 1.

[17] I.A. Schwirtlich and H. Schultz, Philos. Mag. A42 (1980) 601.

[18] G. Duesing, W. Sassin, W. Schilling, H. Hemmerich, Crystal Lattice Defects, v. 1 (1969), 55.

[19] V. Kh. Alimov, J. Roth, M. Mayer, J.Nucl.Mater., 337-339 (2005) 619.

[20] S. Nagata, K. Takahiro, J.Nucl.Mater., 283-287 (2000) 1038.

[21] R.G. Macaulay-Newcombe, M. Poon, A.A. Haasz, J.W. Davis, Proceedings of 7th International Workshop on Hydrogen Isotopes in Fusion Reactor Materials, May 20-21, 2004, Sebasco Harbor Resort ,USA.

[22] J.P. Biersack and L.G. Haggmark. Nucl. Instrum. and Meth. 174 (1980) 257.

[23] M. Poon, R.G. Macaulay-Newcombe, J.W. Davis, A.A. Haasz, J.Nucl.Mater., 337-339 (2005) 629.

[24] R. Sakamoto, T. Muroga, N. Yoshida, J.Nucl. Mater. 220-222 (1995) 819.

[25] K. Tokunaga, M.J. Baldwin, R.P. Doerner, N. Noda, Y. Kubota, N. Yoshida, T. Sogabe, T. Kato, B. Schedler, J. Nucl. Mater. 337-339 (2005) 887.

[26] W. Eckstein, Computer simulation of ion-solid interaction, Springer Berlin, 1991.

[27] R. Frauenfelder, J. Vac. Sci. Technol. 6 (1968) 388.

[28] M.A. Pick and K.Sonnenberg, J. Nucl. Mater., 131 (1985) 208.

[29] P.W. Tamm and L.D. Schmidt, J. Chem. Phys. 51 (12) (1969) 5352.

Table 1. Energies of deuterium release from W, in eV. Q_c is the heat of chemisorption, Q_s is the heat of solution, E_m is the diffusion barrier, E_b^{dis} is the binding energy of deuterium with a dislocation, E_b^{vac} is the binding energy of deuterium with a vacancy, $E_b^{cluster}$ is the binding energy of deuterium in a deuterium cluster.

Deuterium in atomic form (D)	
From chemisorption sites on the surface	$Q_c=0.4 \div 0.9$
From solution	$E_m=0.4$ eV
From dislocation	$E_t=E_m+E_b^{dis}=0.4+0.45=0.85$
From vacancy	$E_t=E_m+E_b^{vac}=0.4+1.05=1.45$
From chemisorption on internal surface of pore	$E_t=Q_c+Q_s+E_m=(0.4 \div 0.9)+1.04+0.4=1.84\text{-}2.34$
Deuterium in molecular form (D_2)	
From deuterium cluster	$E_t \leq E_m+E_b^{cluster}=0.4+1.05=1.45$
From vacancy cluster (pore)	$E_t \geq E_m+ E_b^{vac}=0.4+1.05=1.45$

Table 2. Parameters of deuterium diffusion with trapping in tungsten for non-activated desorption. W_t is the concentration of traps, E_t is the trap energy and η is the rate of ion-induced defect production.

Diffusivity [27], $D = D_0 \exp(-E_m / kT)$		Recombination coefficient [28,29], $K_r = K_{r0} \exp(-E_r / kT)$		Trapping parameters [9, present work]
D_0(m^2/s)	E_m (eV)	K_{r0} (m^4/s)	E_r (eV)	E_t (eV), W_t(at.fr.)
4.1×10^{-7}	0.39	3×10^{-25}/T$^{1/2}$	-2.06	Low energy intrinsic traps: E_t = 0.85 eV, W_t=3×10^{-4} at.fr.=const High energy intrinsic traps: E_t = 1.45 eV, W_t=10^{-5} at.fr.=const *Ion-induced traps for 200 eV:* E_t = 1.45 eV, W_m=0.05 at.fr., $\eta = 10^{-3}$ E_t = 0.85 eV, W_m=0.001 at.fr., $\eta = 2\times10^{-3}$ *Ion-induced traps for 3000 eV:* E_t = 1.45 eV, W_m=0.002 at.fr., $\eta = 5\ 10^{-3}$ E_t = 0.85 eV, W_m=0.001 at.fr., $\eta = 2$ Diffusion coefficient near the surface increases during implantation according to eq. (3) due to the ion-induced stress field.

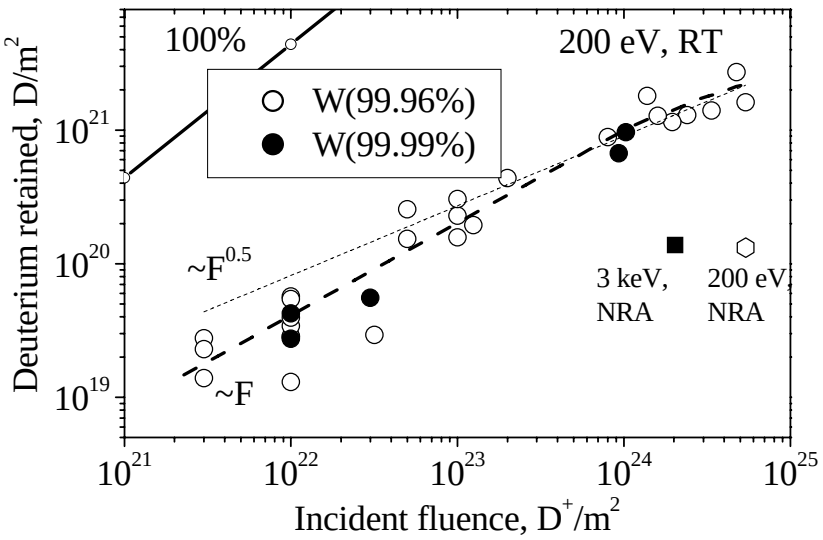

Fig. 1. Fluence dependence of the amount of retained deuterium in PCW (99.96%) and PCW (99.99%) irradiated with 200 eV D^+ at room temperature. The amount of D measured by NRA within a surface layer up to 800 nm for 200 eV and 3 keV is also shown. The reflection coefficient of 200 eV D^+ from tungsten is r=0.56 [26].

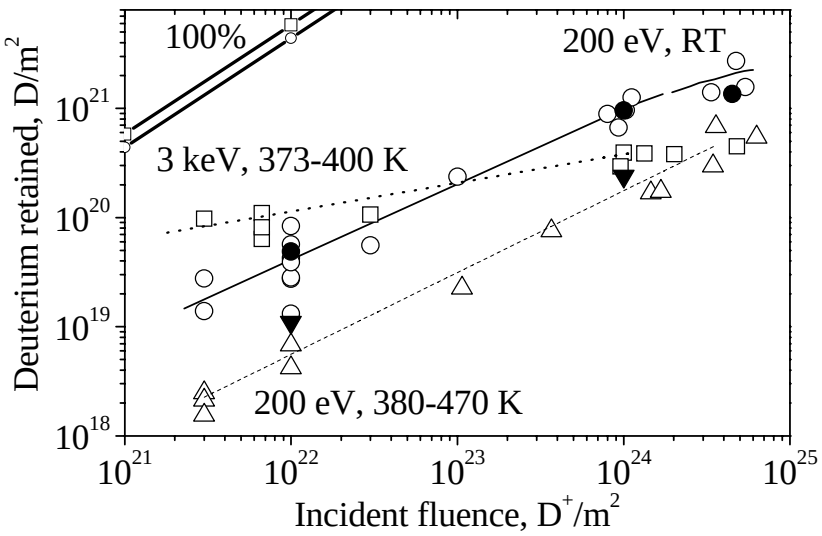

Fig. 2. Fluence dependence of the amount of retained deuterium in PCW irradiated with 200 eV D^+ and 3 keV D^+. The reflection coefficients of 200 eV D^+ and 3 keV D^+ from tungsten are r=0.56 and r=0.417, respectively [26]. Lines are only to guide the eye. Solid circles and solid triangles are calculations for irradiation with 200 eV D^+ at RT and 380-470 K irradiation temperatures, respectively.

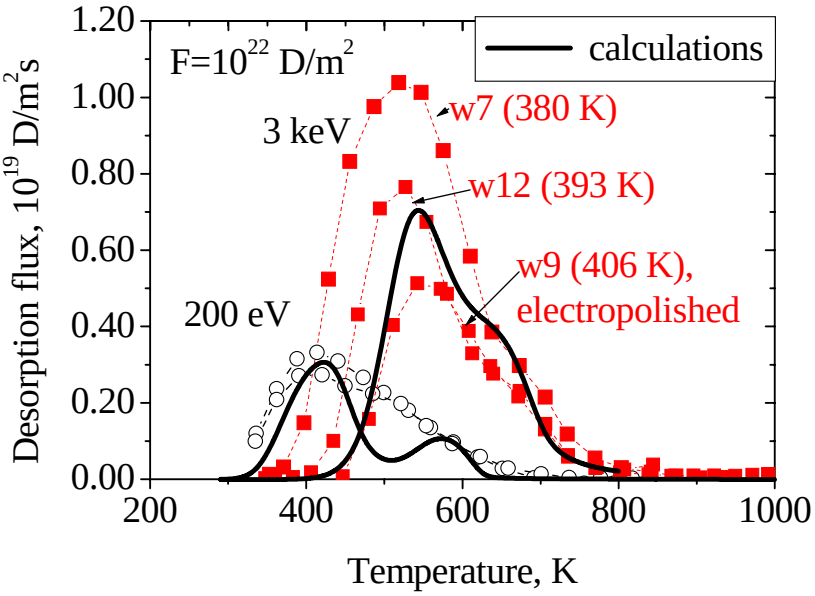

Fig. 3. Experimental thermodesorption spectra of deuterium from polycrystalline W irradiated with 200 eV D^+ (300K) and 3 keV D^+ (400K) for low fluence of $F=10^{22}$ D/m^2. Calculations (solid lines) using the parameters presented in Table 2 are in a good agreement with experiments.

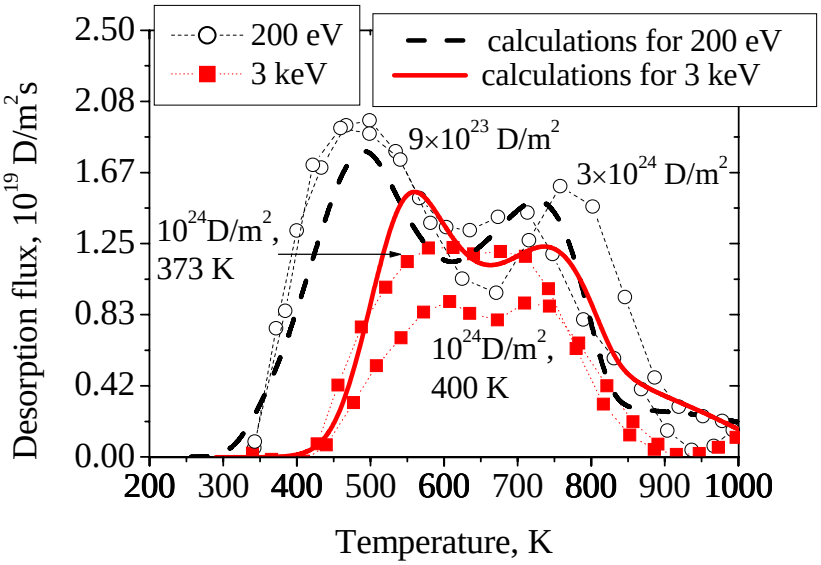

Fig. 4. Experimental thermodesorption spectra of deuterium from polycrystalline W irradiated with 200 eV (300K) and 3 keV (~400K) deuterium ions for high fluence of $F \approx 10^{24}$ D/m^2. Calculations (dashed line for 200 eV and solid line for 3 keV) using the parameters presented in Table 2 are in a good agreement with experiments. Calculations for 200 eV are for room temperature, calculations for 3 keV are at 393 K.

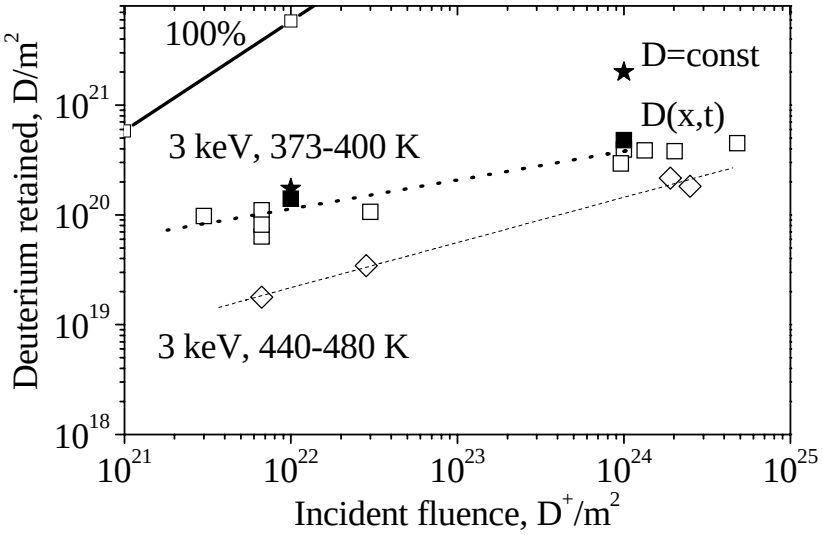

Fig. 5. Experimental (open symbols) and calculated (solid symbols) amounts of retained deuterium fluence in polycrystalline W irradiated with 3 keV D^+as a function of incident fluence. Lines are only to guide the eye. Solid stars are calculations using the model without the change of the diffusion mechanism. Solid squares are calculations using the model including the increase of the diffusion coefficient in the implantation range with fluence and an increase of the speed of the defect production.

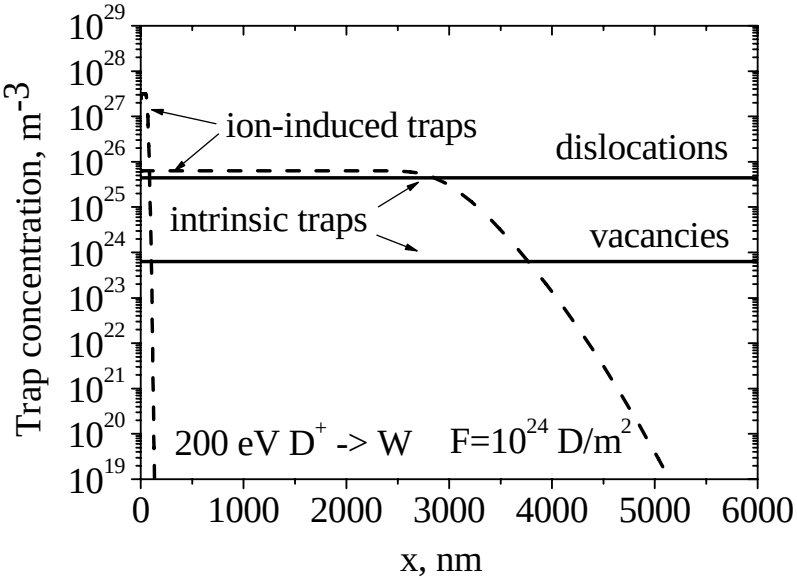

Fig. 6. Depth distribution of traps in polycrystalline W after irradiation with 200 eV D^+ at room temperature up to a fluence of $F=10^{24}$ D/m^2, as used by the model.

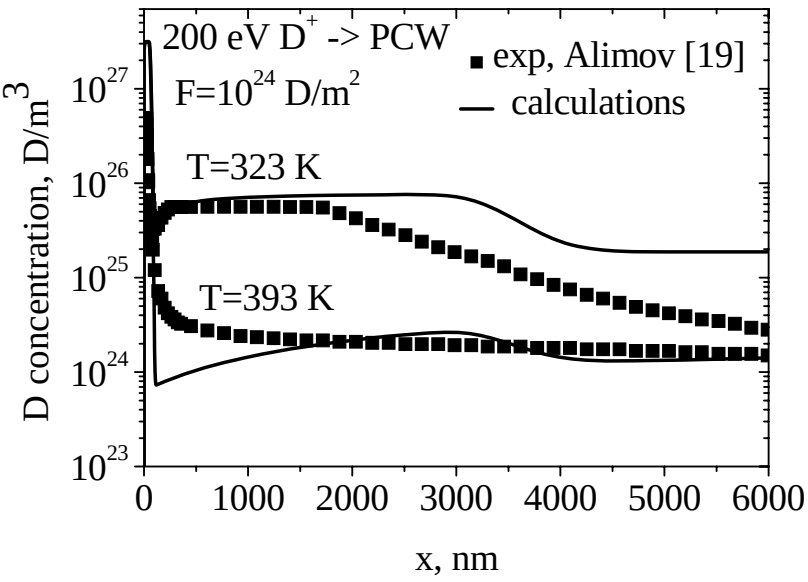

Fig. 7. Calculated and experimental [19] depth profiles of deuterium in polycrystalline W irradiated at 323 K and 393 K with 200 eV D ions up to a fluence of $F=10^{24}$ D/m^2.

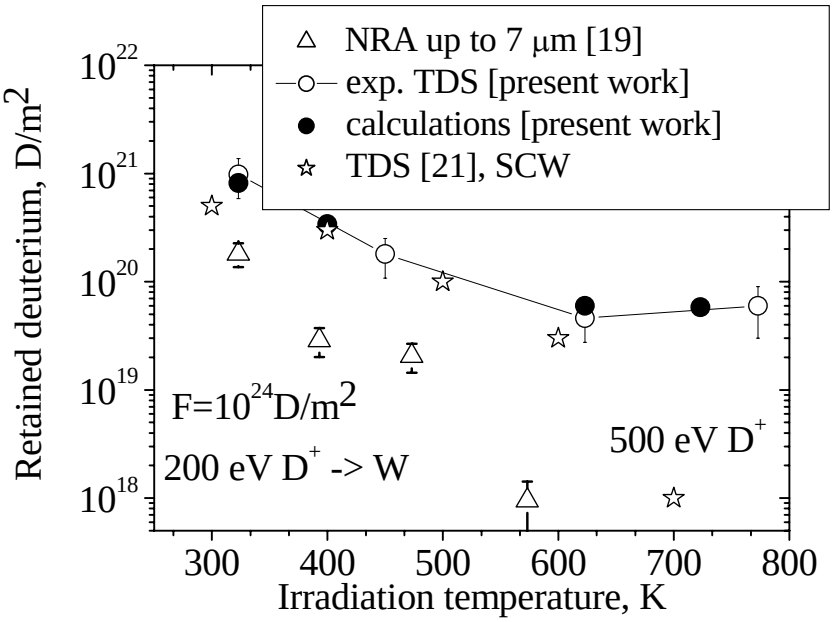

Fig. 8. Deuterium retained in polycrystalline W irradiated with 200 eV D^+ at different temperatures up to a fluence of $F=10^{24}$ D/m^2. Dark solid circles are calculations. Experimental data by Alimov et al. for PCW [19] irradiated with 200 eV D^+ and by R.G. Macaulay-Newcombe et al. for SCW [21] irradiated with 500 eV D^+ are also shown for comparison.

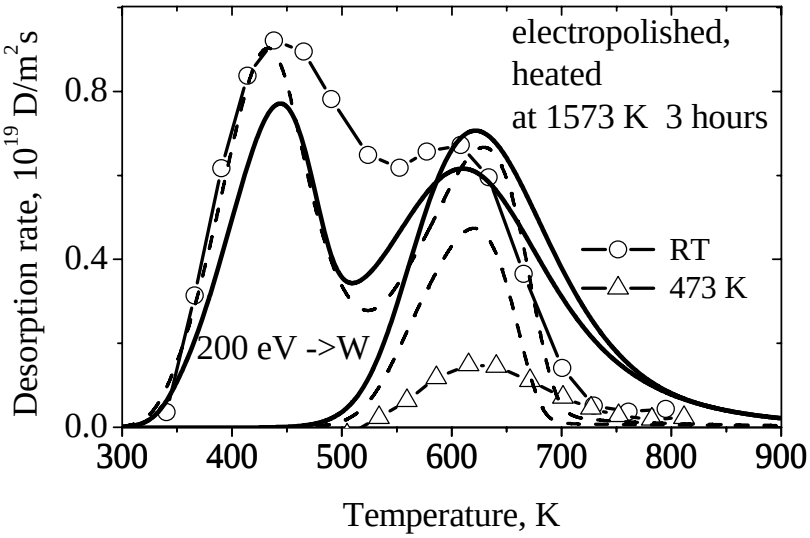

Fig. 9. Experimental thermodesorption spectra of deuterium from polycrystalline W irradiated with 200 eV deuterium ions for fluence of $F=10^{23}$ D/m^2. Dashed lines are calculations using the parameters presented in Table 2 and solid lines are calculations using only 'natural' traps with trapping energies of 0.9 eV and 1.2 eV and trapping densities of $W=10^{-3}$ at.fr. and $W=6\times10^{-4}$ at.fr., respectively.

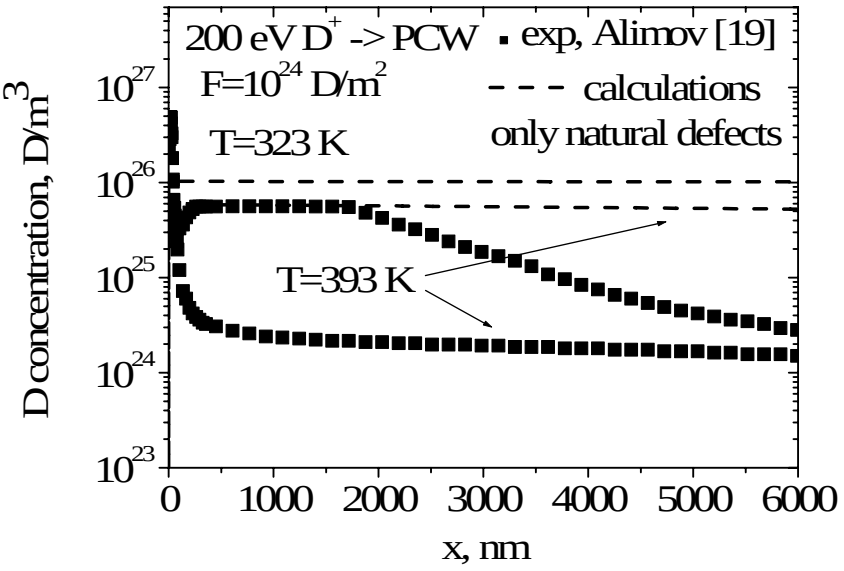

Fig. 10. Calculated and experimental [19] depth profiles of deuterium in polycrystalline W irradiated at 323 K and 393 K with 200 eV D ions up to a fluence of $F=10^{24}$ D/m^2. Calculations are only for 'natural' traps of 0.9 eV with concentration of $W=10^{-3}$ at.fr. and 1.2 eV with concentration of $W=6\times10^{-4}$ at.fr..

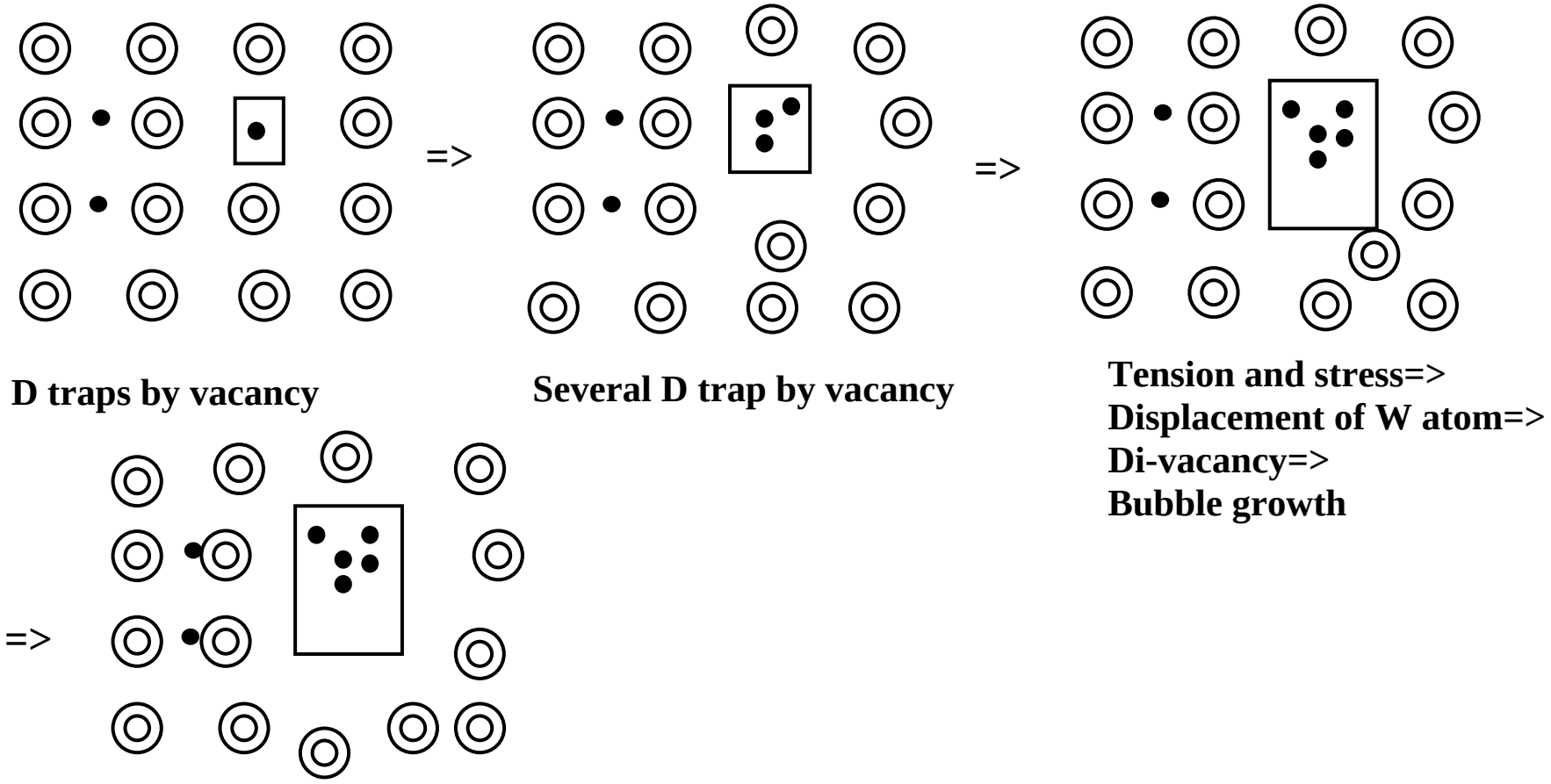

Fig. 11. One posible mechanism of deuterium agglomeration in clusters and bubble growth by atomic deuterium diffusion. Black points are deutereium atoms, squares are vacancies and white atoms are lattice W atoms. Other possible mechanism is the vacancies (or complexes deuterium+vacancy) agglomeration in clusters and finally voids.

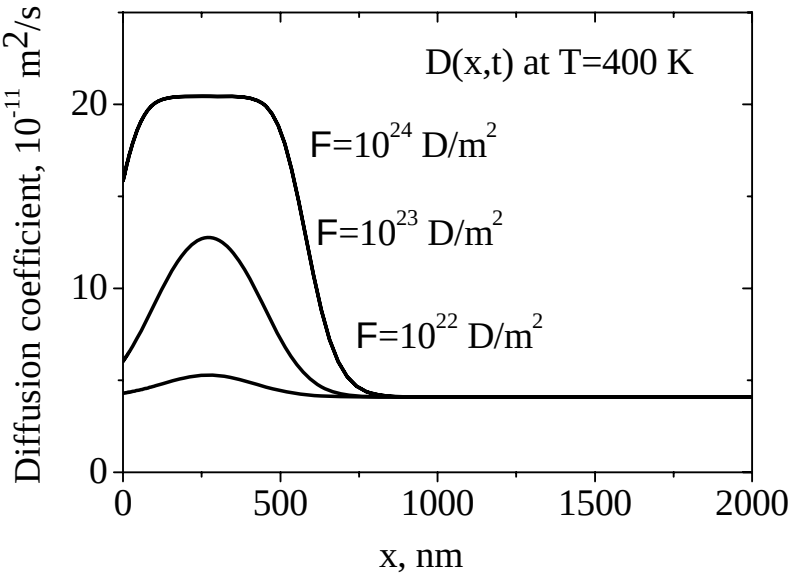

Fig. 12. Diffusion coefficient in PCW near the implanted surface at different fluences for 3 keV D^+ irradiation at 400 K.

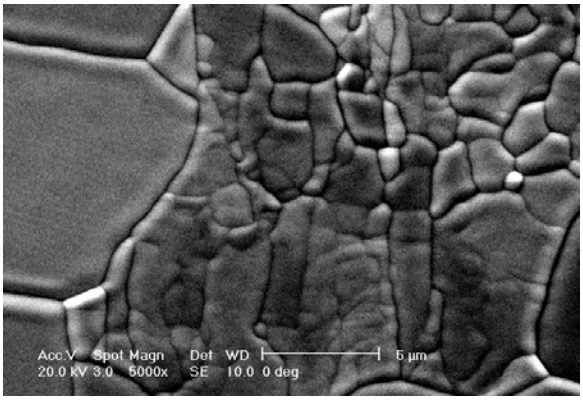

a)

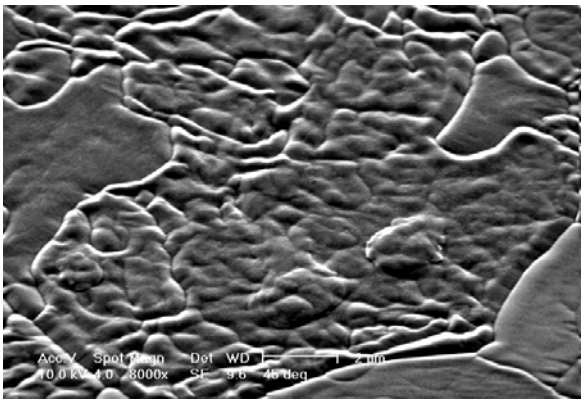

b)

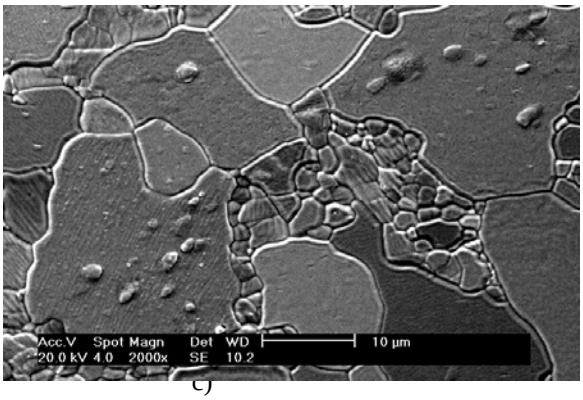

c)

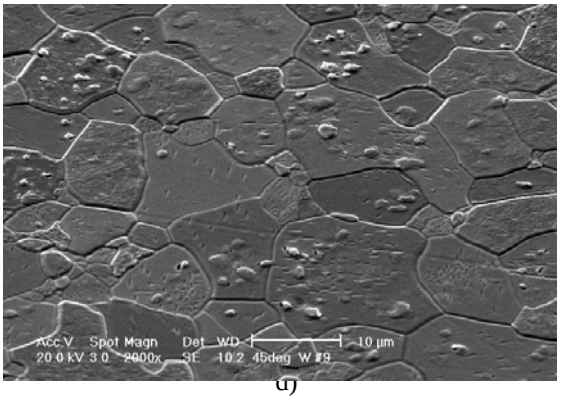

d)

Fig. 13. SEM images of PCW irradiated with 200 eV and 3 keV D^+. The images were obtained after TDS annealing.

a) Virgin (unimplanted) PCW annealed at 1573 K for 3 hours

b) PCW irradiated by 200 eV D^+ at RT up to a fluence of $F=5\times10^{24}$ D/m^2

c) PCW irradiated by 3 keV D^+ at RT (399 K during implantation) up to a fluence of $F=9.5\times10^{23}$ D/m^2

d) PCW irradiated by 3 keV D^+ at RT (393 K during implantation) up to a fluence of $F=1.2\times10^{24}$ D/m^2 and then by 200 eV D^+ at RT up to a fluence of $F=1.94\times10^{24}$ D/m^2.

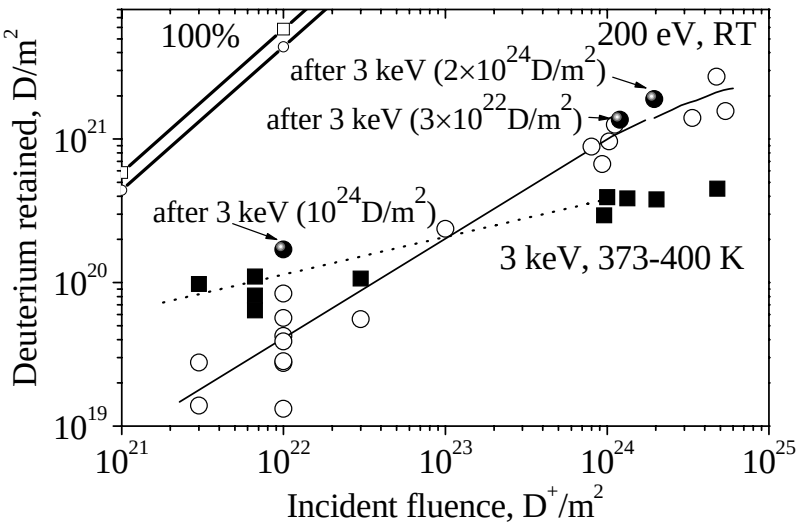

Fig. 14. Pre-implantation effect of 3 keV D^+ at 400 K (and then release of deuterium by TDS) on 200 eV deuterium retention at 300 K in PCW.

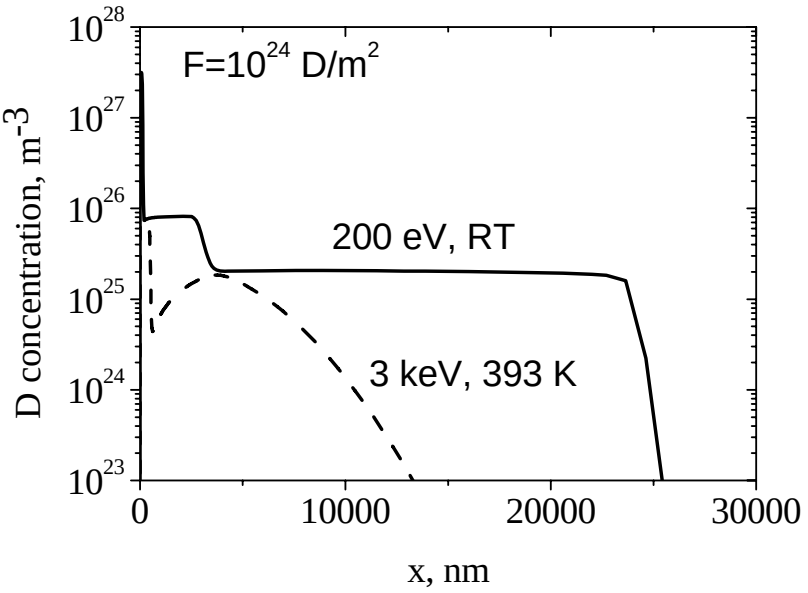

Fig.15. Calculated depth profile of deuterium in W irradiated with 200 eV D^+ and 3 keV D^+ at room temperature and 393 K, respectively, at a fluence of F=10^{24} D/m^2.

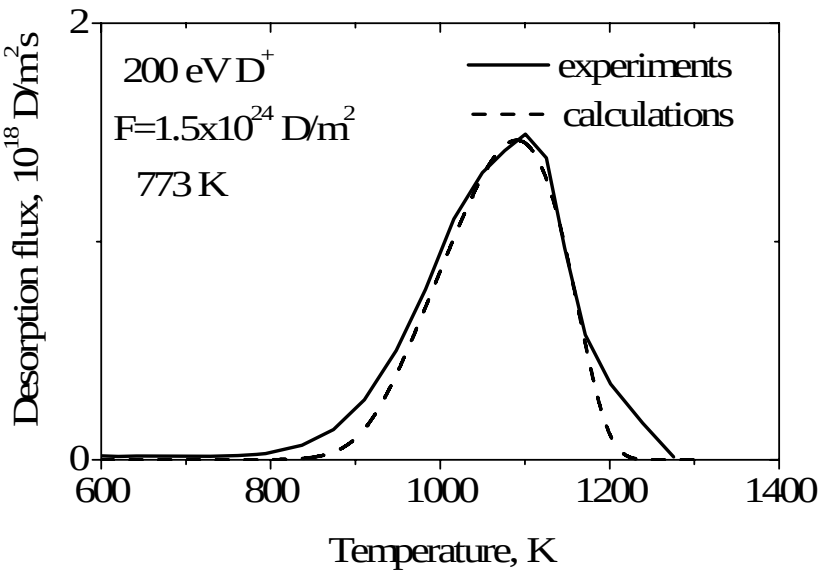

Fig. 16. Experimental thermodesorption spectra of deuterium from un-annealed polycrystalline W irradiated with 200 eV deuterium ions at 773 K for high fluence of $F \approx 10^{24}$ D/m^2. Calculations (dashed line) using the additional traps (voids) with trapping energy of 2.1 eV are in a good agreement with experiments.